

Enhanced transmission from a single subwavelength slit aperture surrounded by grooves on a standard detector

L. A. Dunbar, M. Guillaumée, F. de León-Pérez, C. Santschi, E. Grenet, R. Eckert, F. López-Tejiera, F. J. García-Vidal, L. Martín-Moreno, and R. P. Stanley

Citation: *Applied Physics Letters* **95**, 011113 (2009); doi: 10.1063/1.3160544

View online: <http://dx.doi.org/10.1063/1.3160544>

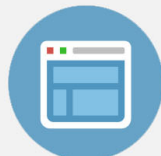
View Table of Contents: <http://scitation.aip.org/content/aip/journal/apl/95/1?ver=pdfcov>

Published by the [AIP Publishing](#)



Re-register for Table of Content Alerts

Create a profile.



Sign up today!



Enhanced transmission from a single subwavelength slit aperture surrounded by grooves on a standard detector

L. A. Dunbar,^{1,a)} M. Guillaumée,¹ F. de León-Pérez,² C. Santschi,¹ E. Grenet,¹ R. Eckert,¹ F. López-Tejiera,² F. J. García-Vidal,³ L. Martín-Moreno,² and R. P. Stanley¹

¹CSEM Centre Suisse d'Electronique et de Microtechnique, Jaquet-Droz 1 SA CH-2002 Neuchâtel, Switzerland

²Departamento de Física de la Materia Condensada and Instituto de Ciencia de Materiales de Aragón (ICMA), CSIC-Universidad de Zaragoza, E-50009 Zaragoza, Spain

³Departamento de Física Teórica de la Materia Condensada, Universidad Autónoma de Madrid, E-28049 Madrid, Spain

(Received 17 March 2009; accepted 9 June 2009; published online 9 July 2009)

An enhanced transmission is detected through a single slit of subwavelength width surrounded by grooves in a gold layer that is added as a postprocess to a standard complementary metal oxide semiconductor (CMOS) fabricated detector. The enhanced transmission results from constructive interference of surface waves, which interact with the incident light. The measured enhanced transmission shows strong qualitative agreement with that predicted by the modal expansion method. With the decreasing dimensions available in standard CMOS process, such nanostructures in metals could be used to replace current optical systems or to improve performance by increasing the signal to noise ratio and/or allowing polarization selection. © 2009 American Institute of Physics. [DOI: 10.1063/1.3160544]

After the first publication on extraordinary transmission,¹ it was shown by Grupp *et al.*² that periodic indentations on the surface could also enhance transmission. This indeed is not surprising given the simple interpretation that constructive interference of surface waves (excited by the grooves) combine in phase with light impinging directly on the slit, increasing the overall light transmission.³ Several papers^{3–5} have presented experimental and theoretical results of corrugated structures on glass or membrane samples. The benefits of high transmission through subwavelength holes have been shown to offer advantages in applications such as high speed detectors at visible wavelengths⁶ and improved signal to noise ratios (S/N) of detectors at midinfrared wavelengths.^{7,8} However, we believe that no work has been done yet on standard detectors in the visible to increase the transmission for improved S/N ratio. Here we show that by a simple postprocessing step on a complementary metal oxide semiconductor (CMOS) fabricated detector, the detected signal can be increased by a factor of more than 8 compared to that of the equivalent detector open surface area. The targeted wavelength for high transmission is 840 nm to target the application of iris detection, which usually takes place between 700–900 nm.⁹ Iris detection would be possible over a larger distance if the detectors had higher S/N ratios. Enhanced transmission by metallic nanostructuring can be directly integrated into CMOS detectors in place of, or in addition to, an expensive lens or the energy-consuming Peltier cooler, which are currently used to increase S/N ratios. Integrating planar metallic nanostructures into commercial detectors is made possible due to the reduced sizes available in CMOS fabrication. In CMOS processing, 90 nm is now standard.

To investigate the optical properties of the metallic nanostructures and their implementation on photodetectors, two sets of samples were fabricated: one on a glass cover slip

(thickness $\sim 150 \mu\text{m}$) and one on the CMOS-fabricated VisionSensor (ViSi) detector.¹⁰ The results on the glass substrate give a clear comparison between theory and experiment allowing us to verify our design tools. The ViSi detector has a pixel size of $50 \times 50 \mu\text{m}^2$ and the active region is $14 \times 14 \mu\text{m}^2$. Figure 1(a) shows an optical image of a portion of the detector array with metallic nanostructures on the active regions. A representation of the fabricated nanostructures is shown in Fig. 1(b). The samples were made by focused ion beam (FIB). Each series of samples consist of a single slit of width $w_{\text{sl}}=100 \text{ nm}$ with 10 grooves. All the grooves have a width and depth of 100 nm ($=h_{\text{gr}}=w_{\text{gr}}$). It should be noted that the control of the slit width is reasonable. The lateral sides of the slit are tilted by 5° . They have a width of 100 nm at the bottom and 115 nm at the top. The control of the depth is difficult and a standard deviation of 20

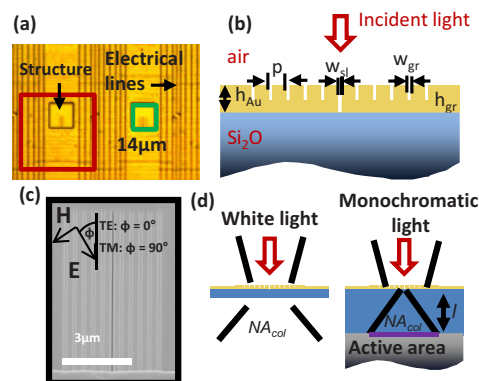


FIG. 1. (Color online) (a) Optical image of an array of pixels on which metal nanostructures have been fabricated by FIB. The red box outlines a pixel (electronics and active area), which is the smallest unit cell. The green box outlines the active (light sensitive) area. The lines outside the active area are for the electronics. (b) Scheme of slit and groove structure. (c) SEM picture of a slit in Au on an active area of a ViSi pixel. The polarization directions are indicated. (d) Scheme of the experimental setups for measuring glass cover slip sample (left) and for detector sample (right).

^{a)}Electronic mail: andrea.dunbar@csem.ch.

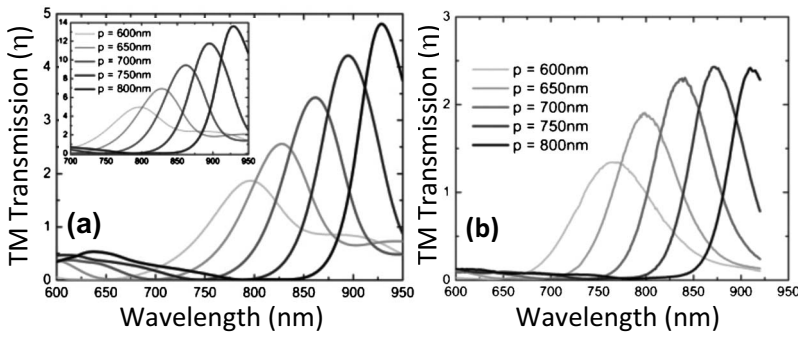


FIG. 2. TM-normalized transmission of a slit and groove structure with parameters $N_{\text{grooves}}=10$, $h_{\text{SiO}_2}=5 \mu\text{m}$, $w_s=100 \text{ nm}$, and $h_g=180 \text{ nm}$. (a) (Inset) Theoretical calculations from the modal expansion method showing the normalized transmission (η). (Inset) Assuming a maximum collection angle (a) η for the collection of the structures on the glass slide. The maximum $\eta=5.0$ when the collection angle $\theta=23.6^\circ$. (b) Experimental values on glass cover slip, the maximum $\eta=3.0$ for the collection angle is $\theta=23.6^\circ$.

nm for the groove depth can be expected with an accuracy of approximately $\pm 15\%$. The length of the slit and grooves is $10 \mu\text{m}$. The period p was varied from 600 to 800 nm in 50 nm steps. The measured Au thickness is 180 nm ($=h_g$). A low sample surface roughness is important to reduce plasmon scattering.¹¹ The root mean square surface roughness of the Au was measured at 0.7 nm (5.1 nm) on the glass sample (detector active area) by atomic force microscopy (not shown). The larger surface roughness on the commercial detector is due to the roughness of the underlying SiO₂ on the detector active area. The structures are planar in nature making them suitable for future integration into the CMOS process. A scanning electron microscope image of a structure on the active region of the vision sensor is shown in Fig. 1(c). Slit structures are polarization sensitive, the high transmission being for TM polarized light. The polarization is defined in Fig. 1(c).

The normalization and thus figure of merit is important when assessing the advantages of emerging science for different technologies. For apertures larger than $(\lambda/2)^2$, the light transmitted is approximately equal to the incident flux on the aperture. The light transmitted by much smaller apertures is less than the incident light impinging on them. A practical figure of merit,¹¹ defined here as η , is then the light transmitted through an aperture normalized to the incident flux on it. η is then calculated by measuring the light transmitted through the slit and normalizing it to the light passing through a larger hole [$\gg (\lambda/2)^2$], which has been normalized to the slit area. An $\eta > 1$ means more light is getting through the slit than is impinging on it, $\eta=2$ means twice the amount of light impinging on the slit is getting through. η will vary depending on the collection angle of the optics, and therefore the theoretical η presented correspond to the light collected for the numerical aperture of the experimental setups.

The transmission spectra of the slit and groove array are resonant at the plasmon modes of the corrugated metal surface. There are two factors that combine to produce these modes: the dielectric function of the metal and the geometry of the groove array.^{3,12} A first order optimization of parameters for enhanced transmission was calculated using the modal expansion (ME) method with surface impedance boundary conditions at all interfaces except those of the lateral walls of both slit and grooves where a perfect metal (PM) was assumed.^{12,13} The optimization takes into account the target wavelength of $\lambda=840 \text{ nm}$ and the fact that the structure must be fabricated in a $14 \times 14 \mu\text{m}^2$ area. The calculations show an η of 14 is possible if all the light coming through the slit could be collected [see the inset in Fig. 2(a)]. Figure 2(a) shows the calculated normalized transmission for

different structures which corresponds to the collection angle of the glass slide. The peaks are due to the constructive interference of the surface plasmons and therefore scale with periodicity.³

The optical setup [see Fig. 1(d)] to measure the transmission of the glass sample consisted of a TM-filtered white halogen source, which illuminates the Au side of the sample with a numerical aperture of smaller than 0.1. The light was then collected through an objective with a collection angle of 23.6° in the glass substrate. The light was spectrally analyzed using a spectrometer with a spectral resolution of $\sim 1 \text{ nm}$ and detected on a liquid N₂-cooled charge-coupled device detector.

The normalized spectra for TM-polarized light for the different periods on the glass slide are shown in Fig. 2(b). There is good qualitative agreement between the theoretical and experimental results. The spectral shift of the emission peak to longer wavelengths with increasing 50 nm periods is approximately 35 nm for both theory and experiment. Moreover the linewidths of the peaks, which narrow toward longer wavelengths are also in good quantitative agreement, with a difference between experiment and theory of $< 10\%$. The theoretical curves are slightly redshifted compared to the measured data. However the agreement is still very good, given the fact that the model is an approximation and that there will be an influence on the resonant wavelength due to the nonverticality of the sidewall.³ The measured normalized transmission is reasonable compared to theory at shorter periods (see Fig. 2). The η values are slightly smaller in the experiment compared to the theory. This difference is attributed to the fact that the FIB may have etched some of the glass at the bottom of the slit. This increased surface roughness can cause scattering. For larger periods, the peaks do not increase as expected and the difference between the theory and experiment increases slightly. This discrepancy is attributed to the fact that here the resonances are stronger and thus more strongly affected by fabrication imperfections.

The experimental setup for measuring the detector consisted of TM-polarized incident light from a supercontinuum white source, which was spectrally filtered to a bandwidth of $\sim 2 \text{ nm}$ and focused onto the detector with a numerical aperture smaller than 0.1. The collection angle of the detector is determined by the size of the active region ($14 \times 14 \mu\text{m}^2$) and the length l and refractive index of the intermediate layer [see Fig. 1(d)]. The length $l=5.5 \mu\text{m}$ is measured directly from a cross section of the sample. The collection angle of the detector is 51.8° .

Calculated (a) and experimentally (b) TM-normalized spectra for the detector are shown in Fig. 3. The experimental results on the detector are noisier than on the glass slide

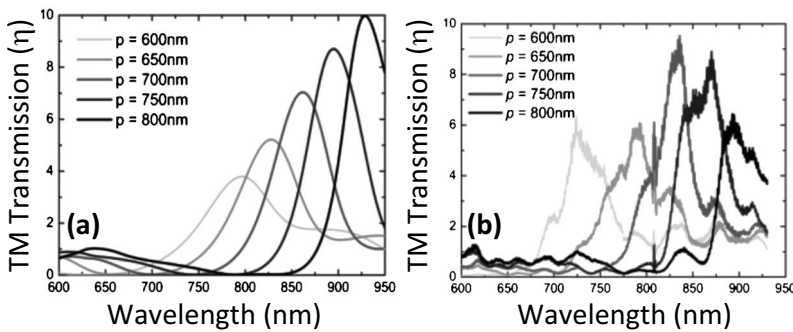


FIG. 3. TM-normalized transmission of slit and groove structure with parameters $N_{\text{grooves}}=10$, $h_{\text{SiO}_2}=5 \mu\text{m}$, $w_s=100 \text{ nm}$, and $h_g=180 \text{ nm}$. (a) Theoretical calculations from the modal expansion method showing the normalized transmission (η) for the structures on the ViSi. The maximum $\eta=10$ for a collection angle $\theta=51.8^\circ$. (b) Experimental values on the ViSi, which shows an $\eta>8.0$ for the collection angle $\theta=51.8^\circ$.

due to the method of detection of the sensor.¹³ The general experimental behavior shows good agreement with that calculated with the ME method, i.e., the redshift of the spectrum with increasing period is reproduced, as are the linewidths. These measurements also show a redshift compared to theoretical results. The larger η in general for the detector when compared to the glass is due to the increased collection angle, 51.8° .

An η , normalized transmission, of greater than eight is measured. This figure is a lower limit as can be seen in the inset in Fig. 2(a) and eta of up to 14 should be achievable. There is a small Fabry-Pérot oscillation imposed on the on the detector data due to the multiple reflections of the light in the SiO₂ layer between the active region and the surface of the detector. This oscillation is not seen on the transmission through the slit in the gold layer as the diffraction from the slit results in many different angles being detected at the detector. This is a real effect and therefore does give a true comparison to the raw data being detected.

The effect of the polarization filtering from the slit geometry is shown in Fig. 4,¹⁴ which show normalized transmission spectra for polarizations between TM and TE. It can clearly be seen that the structure is strongly polarization dependent (the inset shows extinction ratios of >100). This is much less than that predicted for a perfect geometry slit by the ME theory where a value of 35 000 is computed for wavelengths of 800 nm. This discrepancy is unsurprising as the extinction ratio is extremely sensitive to details, such as length of the slit and polarization mixing, which will occur

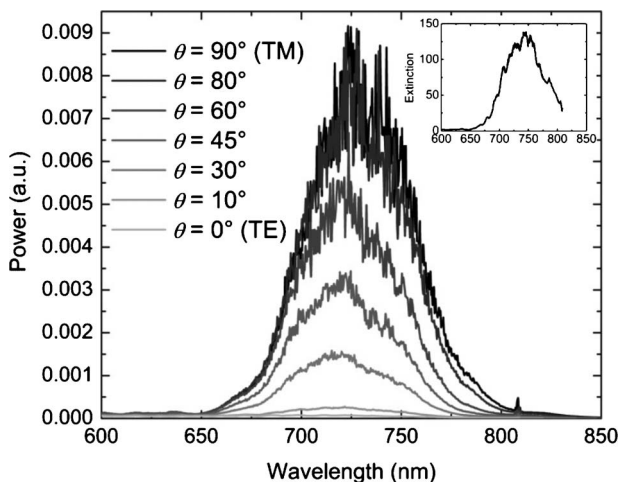


FIG. 4. Nonnormalized polarization dependant transmission spectra of a slit and groove structure on detector. The structure is that which has $p=600 \text{ nm}$. The inset shows the spectrum of the extinction ratio.

due to the nonvertical sidewalls. It should be noted that harvesting structures that spectrally filter but that are not polarization selective can be made by making a circularly symmetric structure, a typical one is the so called bull's-eye structure.¹⁵

In conclusion, we have designed and optically characterized slit and groove structures, and shown good agreement with theory, validating our design method. We transferred this design onto a CMOS detector and have shown an eight times increased optical transmission. The light transmitted was polarization dependant with an extinction ratio of 100. Although Au was used in this study to avoid oxidation effects, numerical simulations (not shown) give comparable enhanced transmissions with aluminum which is the standard metal used in CMOS. This work shows that metallic nanostructures could offer an integrated CMOS solution to provide viable alternative or improved functionality, such as spectral and polarization filtering, increased S/N ration, and improved speed to commercial devices.

We would also wish to thank D. Damjanovic, E. Franzi and P.-F. Rüedi. The work described in this paper was supported by European Project FP6 PLEAS Project No. 034506.

¹T. W. Ebbesen, H. J. Lezec, H. F. Ghaemi, T. Thio, and P. A. Wolff, *Nature (London)* **391**, 667 (1998).

²D. E. Grupp, H. J. Lezec, T. Thio, and T. W. Ebbesen, *Adv. Mater. (Weinheim, Ger.)* **11**, 860 (1999).

³F. J. García-Vidal, H. J. Lezec, T. W. Ebbesen, and L. Martín-Moreno, *Phys. Rev. Lett.* **90**, 213901 (2003).

⁴A. Degiron and T. W. Ebbesen, *Opt. Express* **12**, 3694 (2004).

⁵O. T. A. Janssen, H. P. Urbach, and G. W. 't Hooft, *Phys. Rev. Lett.* **99**, 043902 (2007), and reference therein.

⁶T. Ishi, J. Fujikata, K. Makita, T. Baba, and K. Ohashi, *Jpn. J. Appl. Phys., Part 2* **44**, L364 (2005).

⁷R. D. R. Bhat, N. C. Panoiu, S. T. J. Brueck, and R. M. Osgood, Jr., *Opt. Express* **16**, 4588 (2008).

⁸Z. Yu, G. Veronis, S. Fan, and M. Brongersma, *Appl. Phys. Lett.* **89**, 151116 (2006).

⁹J. Daugman, *IEEE Trans. Circuits Syst. Video Technol.* **14**, 21 (2004).

¹⁰P.-F. Rüedi, P. Heim, F. Kaess, E. Grenet, F. Heitger, P.-Y. Burgi, S. Gyger, and P. Nussbaum, *IEEE J. Solid-State Circuits* **38**, 2325 (2003).

¹¹A. Hoffmann, Z. Lenkefi, and Z. Szentirmay, *J. Phys.: Condens. Matter* **10**, 5503 (1998).

¹²F. López-Tejiera, F. J. García-Vidal, and L. Martín-Moreno, *Phys. Rev. B* **72**, 161405 (2005).

¹³F. de León-Pérez, G. Brucoli, F. J. García-Vidal, and L. Martín-Moreno, *New J. Phys.* **10**, 105017 (2008).

¹⁴Note integration was over a fixed period of time to a fixed voltage. This prevents saturation and gives a large dynamical range. However, the noises scales inversely proportional to signal. This is particularly apparent on Fig. 4.

¹⁵E. Laux, C. Genet, T. Skauli, and T. W. Ebbesen, *Nat. Photonics* **2**, 161 (2008).